IJARCCE ISSN (O) 2278-1021, ISSN (P) 2319-5940

International Journal of Advanced Research in Computer and Communication Engineering

ISO 3297:2007 Certified ⁜ Impact Factor 8.102 ⁜ Peer-reviewed / Refereed journal ⁜ Vol. 12, Issue 5, May 2023

DOI: 10.17148/IJARCCE.2023.12547

SKIN LESION DETECTION FROM DERMOSCOPIC IMAGES USING CASCADED ENSEMBLING OF CNN

Anil Kumar R[1], Sneha N V[2]

Asst. Prof, Dept. of ECE, S.J.C.I.T, Chikkaballapur, India[1]

Dept. of ECE S.J.C.I.T, Chikkaballapur, India[2]

Abstract- Skin cancer is caused due to unusual development of skin cells and deadly type cancer. Early diagnosis is very significant and can avoid some categories of skin cancers, such as melanoma and focal cellcar cinoma. The recognition and the classification of skin malignant growth in the beginning time is expensiveand challenging. The deep learning architectures such as recurrent networks and convolutional neural networks (ConvNets) are developed in the past, which are proven appropriate for non-handcrafted extraction of complex features. To additional expand the efficiency of the ConvNet models, a cascaded ensembled network that uses an integration of ConvNet and handcrafted features based multi-layer perceptron is proposed in thiswork. This offered model utilizes the convolutional neural network model to mine non-handcrafted image features and colour moments and texture features as handcrafted features. It is demonstrated that accuracy ofensembled deep learning model is improved to 98.3% from 85.3% of convolutional neural network model.

Keywords: Project discusses skin lesion colour moment features, texture features, convolution neural network, proposed methodology and image dataset.

I. INTRODUCTION

Skin cancer is a serious and potentially deadly disease that affects millions of people around the world. The most common types of skin cancer are basal cell carcinoma, squamous cell carcinoma, and melanoma. Early detection and diagnosis of skin cancer are crucial for successful treatment and management of the disease. However, skin cancer diagnosis is a challenging task, and can be time- consuming and subjective, even for experienced dermatologists.

In recent years, machine learning techniques have been used to develop automated skin cancer detection systems that can assist dermatologists in making accurate diagnoses. One of the most promising approaches to automated skin cancer detection is the use of deep learning techniques, such as convolutional neural networks (CNNs), which can learn to extract relevant features from skin lesion images and classify them into different categories. However, CNNs alone may not be sufficient for accurate skin cancer detection, as they may miss subtle features or variations in the images that are important for diagnosis. To address this challenge, a cascaded ensembling of CNN and handcrafted features-based deep neural network approach is proposed for dermatologist-level classification of skin cancer The system combines the strengths of CNNs, which can extract high-level features from the images, with handcrafted feature-based deep neural networks, which can extract more complex features and refine the classification. The proposed system has the potential to improve the accuracy and efficiency of skin cancer diagnosis. and could be a valuable tool for dermatologists and other healthcare professionals.

1.1 RELATED WORK

A five-layer CNN has been used for classifying three types of dermatoscopic ailments-melanoma, common nevus and atypical nevus. PH2 data set has been used, and it contains 200 images. Less no. of images is the limitation. Sometimes 100 percent testing accuracy has been noticed. So, dropouts were added while training the model, but the problem of overfitting was persistent [2]. Next implementation consists of the model which uses pretrained Xception architecture with prior imagesegmentation. The upper classifying layers were frozen and new ones were added to classify diseases. The classification of malignant and benign tumours provided eighty-nine percent accuracy [4]. In the implementation of this paper, the images have been classified as benign and malignant, and it consists of 2437 training images, 660 test images and 200 validation images. The model has been implemented using Resnet-101 and Inception-v3 architecture. Resnet has an accuracy of 84.09 percent, also train and loss lines are almost constant after fifty epochs and the training accuracy reaches a saturation point after the fiftieth epoch. Inceptionv3 has an accuracy of 87.42 percent. Here train and

IJARCCE ISSN (O) 2278-1021, ISSN (P) 2319-5940

International Journal of Advanced Research in Computer and Communication Engineering

ISO 3297:2007 Certified ⁜ Impact Factor 8.102 ⁜ Peer-reviewed / Refereed journal ⁜ Vol. 12, Issue 5, May 2023

DOI: 10.17148/IJARCCE.2023.12547

validation accuracy start varying drastically after the fortieth epoch [3]. Next, the authors have proposed their research on MobileNets based on depth wise separable convolutions. The research includes comparison between various Mobile Net models and other models and proves how the MobileNet model is better with respect to size, speed and accuracy. They've also given a method to build short and quick MobileNets by implementing width and resolution multipliers by compromising a small amount of precision to decrease the size and latency [8].

1.2 DATASET

The HAM10000 dataset contains 10,015 images of seven different types of benign and malignant scars, and their abbreviations are labels. The seven types are Melanocytic Nevi, Melanoma, Benign Keratosis-like Lesions, Basal cell carcinoma, Actinic keratoses, Vascular lesions, and Dermatofibroma. Checking the number of images present for each labelled disease has been done. [7]. Maximum number of images are of Melanocytic Nevi, and Dermatofibroma has the least number of images, so class imbalance is prevalent. According to the research done for this paper, only Melanoma, Basal Cell Carcinoma are malignant scars and they should be treated without any delay. Whereas Melanocytic Nevi and Actinic Keratosis may/may not become carcinogenic over a period of time, though a close watch should be kept at them. Benign Keratosis, VascularLesions, and Dermatofibroma are completely harmless and they can be treated by medications

II. RESEARCH METHODOLOGY

2.1 Implementation of CNN Model

Convolutional Neural Network (CNN) is a development of the Multilayer Perceptron (MLP) which is designed to process two-dimensional data. CNN is included in the type of Deep Neural Network because it has a high network depth and has been widely applied to image data [15]. CNN has an architecture as like as neural networks in general, neurons in CNN have a weight, bias, and activation function. CNN architecture as shown in Figure 1, which consists of the convolution layer with ReLU activation, pooling layer as feature extraction layer, and fully connected layer with softmax activationclassification Layer.

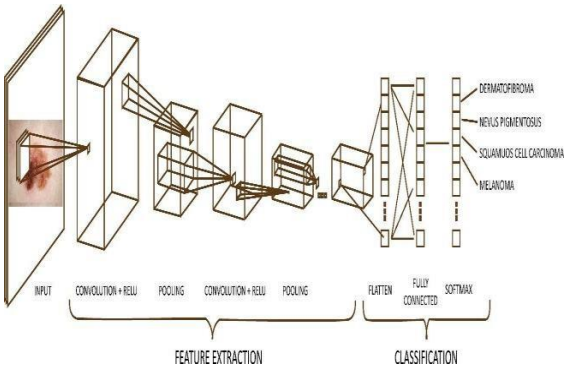

Figure 1. The architecture of CNN

1.1 Convolution Layer

In the Convolution layer, the convolution processis the main process that underlies CNN. Convolution layer is the first layer that will process the image as an input system model. The image will be convoluted with a filter to extract features from the input image that is called the feature map. Figure 2 shows an illustration of the convolutionprocess

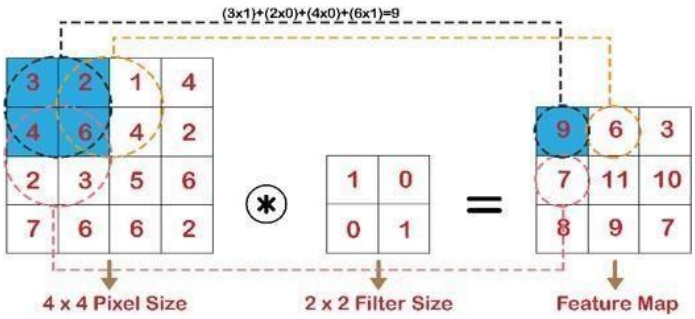

Figure 2. Illustration of the convolution process

International Journal of Advanced Research in Computer and Communication Engineering
ISO 3297:2007 Certified ⁜ Impact Factor 8.102 ⁜ Peer-reviewed / Refereed journal ⁜ Vol. 12, Issue 5, May 2023
DOI: 10.17148/IJARCCE.2023.12547

Activation Rel-U
ReLU (Rectified Linear Unit) is an activation layerin CNN to increase the training stage on neural networks that have advantages to minimize errors. Rel-U activation makes all pixel values to be zero when a pixel image has a value of less than zero [16].

1.2 CONVOLUTION NEURAL NETWORK (CONVNET)

ConvNet is a sort of deep learning architecture that is regularly used to computer vision applications for example object analysis and identification. A ConvNets principally contains convolutional layer, activation layer, dense layer, and pooling layer [42], [43]. ConvNets preserve spatial integrity of input images. Convolution is a mathematical process on two functions that yields a third function that describes how the shape of one is impacted by the other in functional analysis. Both the result function and the method of generating it are referred to as convolution.

The basic purpose of the convolution layer is to extract features from an image. Convolutional kernels are the set of weights that are applied to pixel values. These weights are refined by a back-propagation throughout the learning stage. The convolution operation is applied by convolution kernels.

The continuous domain convolution of two functions f and h is defined as follows [48]. $(f * h)(t) = Z \infty -\infty f(\tau) h(t - \tau)d\tau = Z \infty -\infty f(t - \tau) h(\tau)d\tau$ (15) The analogous convolution operation for discrete signals is defined by: $(f * h)(n) = X\infty m=-\infty f(m) h(n - m) = X\infty m=-\infty f(n - m) h(m)$ (16) This $1 - D$ convolution for $2 - D$ convolution situation is defined by: $(f * h)(x, y)= X M m=-M X N n=-N f(x-n, y-m) h(n, m)$ (17)

The function h is referred to as a filter (kernel) in this case, and it is utilised to convolve over the picture f. The convolution between the kernel and image is achieved at each pixel position and the output is a $2 - D$ array which is termed as feature map.

A nonlinear activation layer for example softmax, Rectified Linear Unit (ReLU) Arbitraryized Leaky Rectified Liner Unit (RL − ReLU), Leaky Rectified Liner Unit (L-ReLU), Parameterized Rectified Liner Unit (P − ReLU), and Exponential Linear Units (ELU) are used activate the output of convolution layer. Activation functions are an essential element of deep learning models [48]. These functions are used to decide the output of a model, accuracy, and also impact on the efficiency of the model. These functions impacts on the convergence and the convergence speed.

A pooling layer is frequently placed after the convolutional layer. Spatial pooling used for down-sampling while preserving the most substantial features. It reduces the number of parameters to avoid overfitting. Various examples of pooling operations are max pooling, average pooling and sum pooling etc. It is also possible to specify the stride and the kernel size in addition to choosing different pooling filters. The final layer is referred as dense layer which is a dense layer. This layer offers the prediction of the ConvNet model.

1.3 PROPOSED CASCADED ENSEMBLED DEEP LEARNING MODEL

A cascaded ensembled deep learning model by integration of handcrafted feature mining and ConvNet learning ability to categorize skin lesions is proposed in this work. A graphical description of the network architecture is presented in Figure 1.

IJARCCE ISSN (O) 2278-1021, ISSN (P) 2319-5940

International Journal of Advanced Research in Computer and Communication Engineering

ISO 3297:2007 Certified ⁜ Impact Factor 8.102 ⁜ Peer-reviewed / Refereed journal ⁜ Vol. 12, Issue 5, May 2023

DOI: 10.17148/IJARCCE.2023.12547

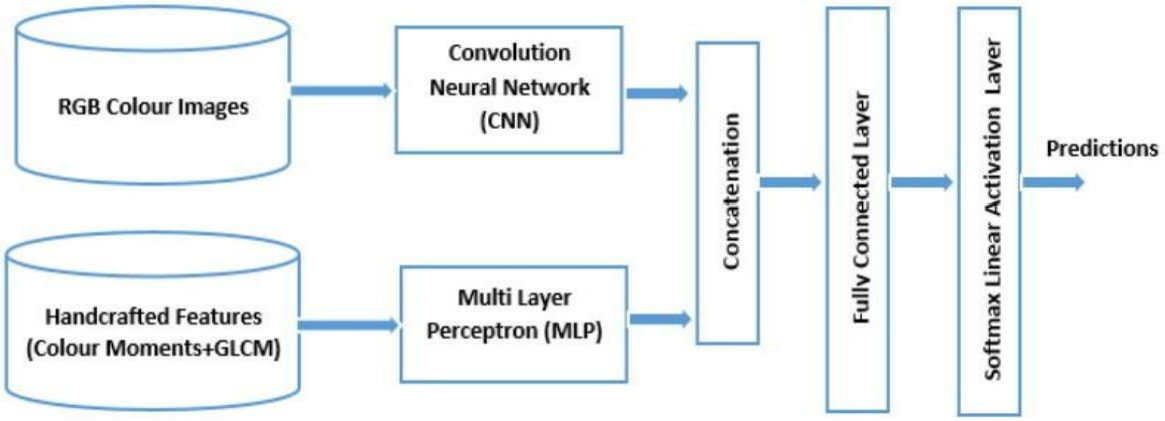

FIGURE 1. Proposed cascaded ensembled deep learning model has one branch that accepts the extracted features as numerical data and another branch that accepts colour images

The cascaded ensembled deep learning model has a dense model and a ConvNet architecture. It has two inputs which are the feature set consisting of colour moments and GLCM features and RGB colour images. A four layer fully connected model is applied to categorize the designated features, that delivers a nonlinear mapping function f (·), which transforms x to y. This mapping is defined as [42] y = f (wx + b) (18) Here, w and b symbolize the weight matrix and bias vector respectively.

The ConvNet is utilized to categorize skin disease images where deep features are mined by convolution layer. The convolutional layers perform convolution in its place of multiplication in the dense layers that is calculated as yj = f X i∈N cij ∗ xi + bj (19) where, N, i, j symbolizes the size of kernel, feature map, and convolution filter respectively. cij is the convolution filter for the i − th input and the j − th output. The outputs of the ConvNet model and fully connected model are consolidated at the last. A softmax transformation function is used here to transform the real values into estimated probability. It is defined as σi = ωxi + b (20) pi = e σi P i e σi (21) where, xi and pi represents the i − th output and the output of the softmax nonlinear activation function respectively. E. IMAGE DATASET Dermoscopic lesion images were acquired from HAM10000 Dataset collected by multiple institutions [45], [46]. It contains 10015 images of skin pigments which are divided amongst seven classes. A disease label for each image are decided diagnostically or histopathologically. This dataset consists of 10, 015, 193, and 1, 512 labelled images in training, validation and test set respectively.

A brief description of each class is given below.

1) ACTINIC KERATOSES (AKIEC) In this category irregular, scaly patches on the skin are assumed to be precancerous. These are mostly appeared owing to sun exposure. 327 images are available in this class.
2) BASAL CELL CARCINOMA (BCC) It is the utmost frequent class of skin cancer that generally appears as a sore that appears to become recovered and then reappears and may start to bleed. These tumours are locally invasive and tend to burrow in but not spread to distant locations. 514 images are available in this class.
3) BENIGN KERATOSIS (BKL) Benign also referred as Lichen planus-like keratosis (LPLK). These lesions normally appear as a single macule, papule, or marker that changes over time as it heals. This class has a total of 1099 scans.
4) DERMATOFIBROMA (DF) It is a frequent benign fibrous nodule that frequently appears on the lower legs and also referred as cutaneous fibrous histiocytoma. This class consists of 115 images.
5) MELANOMA (MEL) It is a severe type of skin cancer, which starts in cells known as melanocytes. It is less frequent than basal cell carcinoma and squamous cell carcinoma however more unsafe because of it spread more rapidly. 1113 images are available in this class.
6) MELANOCYTIC NEVI (NV) Melanocytic nevi are hamartomas or benign neoplasms composed of melanocytes. These are pigment-generating cells. Moles appear throughout early age. These moles grows gradually, change colour, and becomes outstretched. This class consists of 6705 images.
7) VASCULAR SKIN LESIONS (VASC) These are comparatively common irregularities of the skin and tissues. These are generally termed as birthmarks. Vascular tumours may be benign or malignant and can appear anywhere in part of body. This class consists of 114 images.

IJARCCE ISSN (O) 2278-1021, ISSN (P) 2319-5940

International Journal of Advanced Research in Computer and Communication Engineering

ISO 3297:2007 Certified ⁜ Impact Factor 8.102 ⁜ Peer-reviewed / Refereed journal ⁜ Vol. 12, Issue 5, May 2023

DOI: 10.17148/IJARCCE.2023.12547

This dataset has the challenge of learning with imbalanced dataset. This problem is addressed by oversampling of the minority class. A type of data augmentation method referred as the Synthetic Minority Oversampling Technique (SMOTE) is utilized for the minority classes. SMOTE is designed to learn the topological qualities of the neighbourhood of those points in the minority class, making overfitting less likely. This oversampling method first chooses a minority class exampleI1 at arbitrary and recognizes its k closest lesser class neighbours. The synthetic case is then designed by selecting one of the k closest neighbours I2 at arbitrary and connecting I1 and I2 to create a line segment in the feature space. The artificial cases are created as a convexgrouping of the two selected cases I1 andI2.

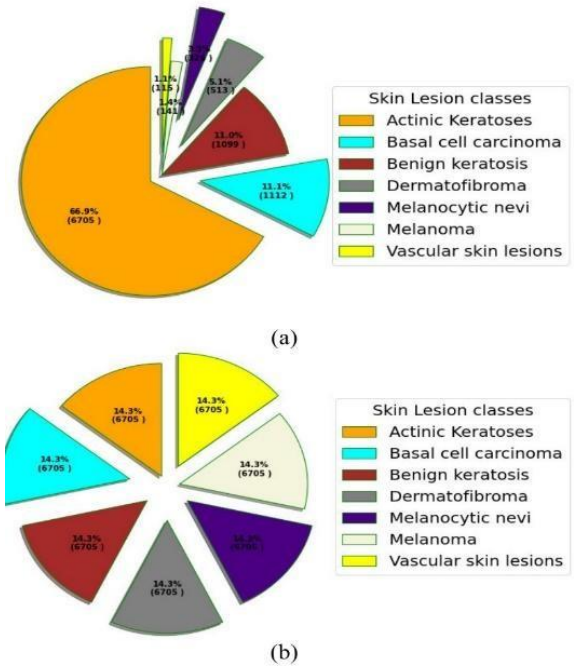

FIGURE 2. Number of images in dataset for each class (a) original dataset and(b) dataset after SMOTE data augmentation

Figure 2 displays the number of images before and after augmentation, whereas Figure 3 displays representative images from all classes. The parameters of SMOTE namely sampling strategy, arbitrary state, shrinkage are set to default values i.e. auto, none and none respectively.

IV. RESULTS

The goal of this study is to evaluate both a ConvNet and a cascaded ensembled deep learning model's generalisation skills. After learning of the classifiers, the performance of each model is assessed using the significant metrics namely precision, sensitivity, f-score and accuracy [41]. Receiver Operating Characteristic (ROC) curves are also computed and displayed to compare and verify the performance of each model.

An ROC graph is a method for envisioning, forming and choosing classifiers based on their precision [42]. It is a 2 − D representation for performance of classifier. However, it is required to reduce ROC dimension to a single scalar quantity for comparison of multiple classifiers. For this purpose, a common metric area under the ROC curve is computed termed as the AUC. Here, AUC is a share of the area of the unit square. AUC ranges between 0 and 1.0. A arbitrary classifier yields the diagonal line between bottom left corner and top right corner, which has an area of 0.5. So, a trained classifier should not have an AUC less

IJARCCE ISSN (O) 2278-1021, ISSN (P) 2319-5940

International Journal of Advanced Research in Computer and Communication Engineering

ISO 3297:2007 Certified ⁜ Impact Factor 8.102 ⁜ Peer-reviewed / Refereed journal ⁜ Vol. 12, Issue 5, May 2023

DOI: 10.17148/IJARCCE.2023.12547

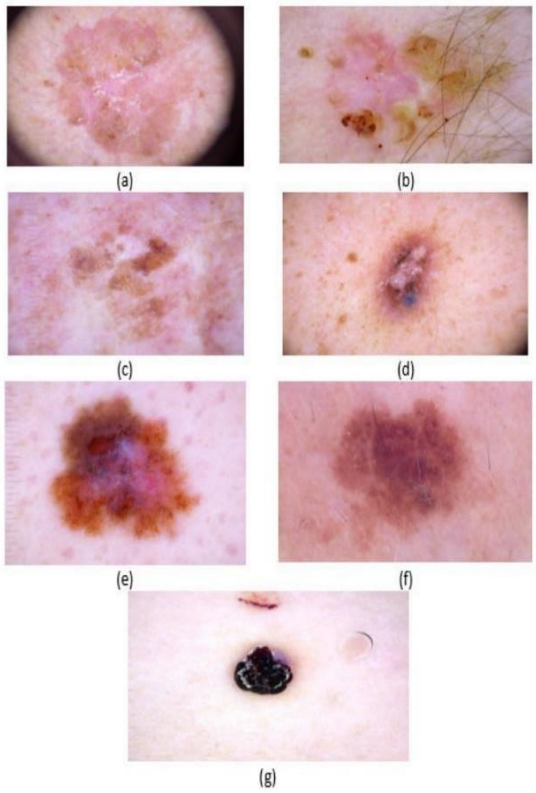

FIGURE 3. Sample images from each seven classes (a) akiec, (b) bcc, (c) bkl, (d) df, (e) Melanoma, (f) mel, and (g) vasc

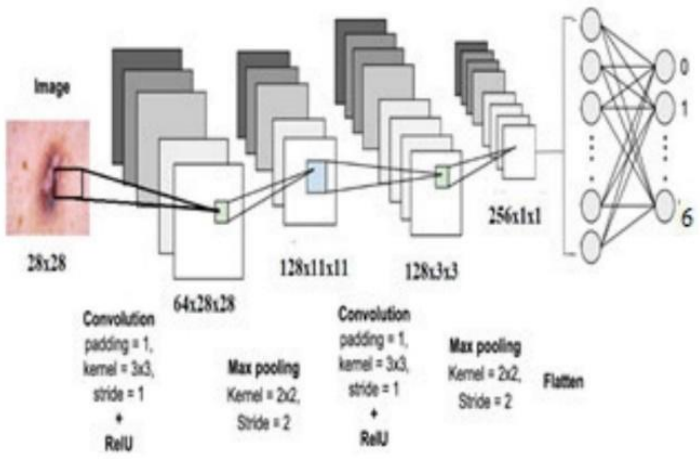

FIGURE 4. ConvNet architecture for skin lesion classification.

than 0.5. AUC value more than 0.95 is considered decent in medical applications. Furthermore, micro average and macro average are computed in this multiclass classification problem. A macro-average metric assesses performance for each skin disease class independently before calculating the mean by taking all classes into account equally, whereas a micro-average metric averages all skin classes to calculate the average value.

APPLICATIONS

1. Early Detection: Early detection is crucial for effective treatment of skin cancer. The technology can help in detecting skin cancer at an early stage, thereby improving the chances of successful treatment.
2. Diagnosis: Dermatologists can use the technology to accurately diagnose skin cancer. It can also aid in

International Journal of Advanced Research in Computer and Communication Engineering
ISO 3297:2007 Certified ⁜ Impact Factor 8.102 ⁜ Peer-reviewed / Refereed journal ⁜ Vol. 12, Issue 5, May 2023
DOI: 10.17148/IJARCCE.2023.12547

distinguishing between different types of skin cancers, such as melanoma and non-melanoma skin cancers.
3. Screening: The technology can be used for mass screening programs to identify individuals who may be at risk for skin cancer. This can help in identifying individuals who require further testing and treatment.
4. Telemedicine: The technology can be used in telemedicine applications to provide remote diagnosis and consultation to individuals who are unable to access dermatological care.

ADVANTAGES

1. High Accuracy: The technology has been shown to achieve dermatologist-level accuracy in the classification of skin cancer, making it a powerful tool for diagnosis and screening.
2. Automation: The technology can automate the process of skin lesion analysis, which can save time and reduce the workload of dermatologists.
3. Objective Results: The technology can provide objective results, which can reduce the subjectivity associated with visual inspection by dermatologists.
4. Cost-Effective: The technology can be a cost-effective
solution for skin cancer diagnosis and screening, particularly in regions with limited access to dermatologists.
5. Scalability: The technology can be easily scaled to handle a large number of skin lesion images, making it suitable for mass screening programs.

CONCLUSION

Considering the current achievement of deep learning architectures, an efficient method is presented for the skin lesion classification. In this work, a cascaded model is created that combines the strengths of models based on hand-crafted feature extraction approaches and deep learning model. To gain the high accuracy of the skin disease image classification the powerful ability of feature learning of deep ConvNets is integrated with handcrafted features including colour moments and texture features. This deep learning architecture termed as cascaded ensembled deep learning model in this paper. The simulation results show that our proposed model outperforms the ConvNet model. More research is being done to create a more robust model by combining clinical features like sex, age, itching, burns, medical history, and location with handmade features to create a more robust model.

CODE AVAILABILITY

For assistance of dermatologist and researchers the code is provided on Github repository at:
https://github.com/shamiktiwari/Skin-cancer- classification-using-CascadedEnsemble-of-ConvNet- and-Handcrafted-Features.

REFERENCES

[1] D. Didona, G. Paolino, U. Bottoni, and C. Cantisani, ‘‘Non melanoma skin cancer pathogenesis overview,’’ Biomedicines, vol. 6, no. 1, p. 6, Jan. 2018.
[2] T. J. Brinker, A. Hekler, J. S. Utikal, N. Grabe, D. Schadendorf, J. Klode, C. Berking, T. Steeb, A. H. Enk, and C. von Kalle, ‘‘Skin cancer classification using convolutional neural networks: Systematic review,’’ J. Med. Internet Res., vol. 20, no. 10, Oct. 2018, Art. no. e11936.
[3] P. Tschandl, C. Rinner, Z. Apalla, G. Argenziano,N. Codella, A. Halpern, M. Janda, A. Lallas, C. Longo,
J. Malvehy, J. Paoli, S. Puig, C. Rosendahl, H. Peter Soyer, I. Zalaudek, and H. Kittle, ‘‘Human–computer collaboration for skin cancer recognition,’’ Nature Med. vol. 26, no. 8, pp. 1229–1234, 2020.
[4] B. C. Baumann, K. M. MacArthur, J. D. Brewer, W. M. Mendenhall, C. A. Barker, J. R. Etzkorn, N. J. Jellinek, J. F. Scott, H. A. Gay, J. C. Baumann, F. A. Manian, P. M. Devlin, J. M. Michalski, N. Y. Lee, W.
L. Thorstad, L. D. Wilson, C. A. Perez, and C. J. Miller, ‘‘Management of primary skin cancer during a pandemic: Multidisciplinary recommendations,’’ Cancer, vol. 126, no. 17, pp. 3900–3906, Sep. 2020.
[4] J. Höhn et al., ‘‘Combining CNN-based histologic whole slide image analysis and patient data to improve skin cancer classification,’’ Eur. J. Cancer, vol. 149, pp. 94–101, May 2021.
[5] C. A. Hartanto and A. Wibowo, ‘‘Development of mobile skin cancer detection using faster R-CNN and MobileNet v2 model,’’ in Proc. 7th Int. Conf. Inf. Technol., Comput., Electr. Eng. (ICITACEE), Sep. 2020, pp. 58–63.
[6] M. A. Kassem, K. M. Hosny, R. Damaševičius, and
M. M. Eltoukhy, ‘‘Machine learning and deep learning methods for skin lesion classification and diagnosis: A systematic review,’’ Diagnostics, vol. 11, no. 8, p. 1390, Jul. 2021.
[7] O. O. Abayomi-Alli, R. Damaševičius, S. Misra, R. Maskeliunas, and A. Abayomi-Alli, ‘‘Malignant skin melanoma detection using image augmentation by oversampling in nonlinear lower-dimensional embedding manifold,’’

DOI: 10.17148/IJARCCE.2023.12547

TURKISH J. Electr. Eng. Comput. Sci., vol. 29, nos. SI–1, pp. 2600–2614, Oct. 2021.

[8] T. C. Pham, V. D. Hoang, C. T. Tran, M. S. K. Luu,
D. A. Mai, A. Doucet, and C. M. Luong, ''Improving binary skin cancer classification based on best model selection method combined with optimizing full connected layers of deep CNN,'' in Proc. Int. Conf. Multimedia Anal. Pattern Recognit. (MAPR), Oct. 2020, pp. 1–6.

[9] N. Hameed, A. Ruskin, K. Abu Hassan, and M. A. Hossain, ''A comprehensive survey on image-based computer aided diagnosis systems for skin cancer,'' in Proc. 10th Int. Conf. Softw., Knowl., Inf. Manage. Appl. (SKIMA), 2016, pp. 205–214.

[10] R. J. Friedman, D. S. Rigel, and A. W. Kopf, ''Early detection of malignant melanoma: The role of physician examination and self-examination of the skin,'' CA, A Cancer J. Clinicians, vol. 35, no. 3, pp. 130–151, May 1985.

[11] N. R. Abbasi, H. M. Shaw, D. S. Rigel, R. J. Friedman, W. H. McCarthy, I. Osman, A. W. Kopf, and
D. Polsky, ''Early diagnosis of cutaneous melanoma: Revisiting the ABCD criteria,'' J. Amer. Med. Assoc.,
vol. 292, no. 22, pp. 2771–2776, Dec. 2004.

[12] J. D. Jensen and B. E. Elewski, ''The ABCDEF rule: Combining the ''ABCDE rule'' and the ''ugly duckling sign'' in an effort to improve patient self- screening examinations,'' J. Clin. Aesthetic Dermatol., vol. 8, no. 2, p. 15, 2015.

[13] F. Ercal, A. Chawla, W. V. Stoecker, H.-C. Lee, and R. H. Moss, ''Neural network diagnosis of malignant melanoma from color images,'' IEEE Trans. Biomed. Eng., vol. 41, no. 9, pp. 837–845, Sep. 1994.

[14] J. F. Alcon, C. Ciuhu, W. T. Kate, A. Heinrich, N. Uzunbajakava, G. Krekels, D. Siem, and G. de Haan, ''Automatic imaging system with decision support for inspection of pigmented skin lesions and melanoma diagnosis,'' IEEE J. Sel. Topics Signal Process., vol. 3, no. 1, pp. 14–25, Feb. 2009.

[15] A. Karimian, M. Ramezani, and P. Moallem, ''Automatic detection of malignant melanoma using macroscopic images,'' J. Med. Signals Sensors, vol. 4, no. 4, p. 281, 2014.

[16] R. Garnavi, M. Aldeen, and J. Bailey, ''Computer- aided diagnosis of melanoma using border- and wavelet-based texture analysis,'' IEEE Trans. Inf. Technol. Biomed., vol. 16, no. 6, pp. 1239–1252, Nov. 2012.

[17] A. Karimian, M. Ramezani, and P. Moallem, ''Automatic detection of malignant melanoma using macroscopic images,'' J. Med. Signals Sensors, vol. 4, no. 4, p. 281, 2014. 17930 VOLUME 10, 2022 A. K. Sharma et al.: Dermatologist-Level Classification of Skin Cancer

[18] A. Romero-Lopez, X. Giro-i-Nieto, J. Burdick, and
O. Marques, ''Skin lesion classification from dermoscopic images using deep learning techniques,'' in Proc. 13th IASTED Int. Conf. Biomed. Eng. (BioMed), 2017, pp. 49–54.

[19] F. Xie, H. Fan, Y. Li, Z. Jiang, R. Meng, and A. C. Bovik, ''Melanoma classification on dermoscopy images using a neural network ensemble model,'' IEEE Trans. Med. Imag., vol. 36, no. 3, pp. 849–858, Mar. 2016.

[20] Z. Yu, D. Ni, S. Chen, J. Qin, S. Li, T. Wang, and
B. Lei, ''Hybrid dermoscopy image classification framework based on deep convolutional neural network and Fisher vector,'' in Proc. IEEE 14th Int. Symp. Biomed. Imag. (ISBI), Apr. 2017, pp. 301–304.

[21] N. C. F. Codella, Q.-B. Nguyen, S. Pankanti, D. A. Gutman, B. Helba, A. C. Halpern, and J. R. Smith, ''Deep learning ensembles for melanoma recognition in dermoscopy images,'' IBM J. Res. Develop., vol. 61,no. 4/5, pp. 5:1–5:15, Jul. 2017. [23] F. Nunnari and D. Sonntag, ''A CNN toolbox for skin cancer classification,'' 2019, arXiv:1908.08187.

[24] S. Mukherjee, A. Adhikari, and M. Roy, ''Malignant melanoma classification using cross- platform dataset with deep learning ConvNets architecture,'' in Recent Trends in Signal and Image Processing. Singapore: Springer, 2019, pp. 31–41.

[25] A. Mahbod, G. Schaefer, C. Wang, R. Ecker, and
I. Ellinge, ''Skin lesion classification using hybrid deep neural networks,'' in Proc. IEEE Int. Conf. Acoust., Speech Signal Process. (ICASSP), May 2019, pp. 1229– 1233.

[26] Q. Abbas and M. E. Celebi, ''DermoDeep—A classification of melanomanevus skin lesions using multi-feature fusion of visual features and deep neural network,'' Multimedia Tools Appl., vol. 78, no. 16, pp. 23559–23580, Aug. 2019.

[27] M. A. Khan, M. Sharif, T. Akram, S. A. C. Bukhari, and R. S. Nayak, ''Developed Newton- Raphson based deep features selection framework for skin lesion recognition,'' Pattern Recognit. Lett., vol. 129, pp. 293–303, Jan. 2020.

[28] K. Polat and K. Onur Koc, ''Detection of skin diseases from dermoscopy image using the combination of convolutional neural network and oneversus-all,'' J. Artif. Intell. Syst., vol. 2, no. 1, pp. 80–97, 2020.

[29] D. Połap, A. Winnicka, K. Serwata, K. Ke¸sik, and
M. Woźniak, ''An intelligent system for monitoring skin diseases,'' Sensors, vol. 18, no. 8, p. 2552, Aug. 2018.

[30] S. Kadry, D. Taniar, R. Damasevicius, V. Rajinikanth, and I. A. Lawal, ''Extraction of abnormal skin lesion from dermoscopy image using VGGSegNet,'' in Proc. 7th Int. Conf. Bio Signals, Images, Instrum. (ICBSII), Mar. 2021, pp. 1–5.

[31] M. A. Khan, T. Akram, Y.-D. Zhang, and M. Sharif, ''Attributes based skin lesion detection and recognition: A mask

DOI: 10.17148/IJARCCE.2023.12547

RCNN and transfer learningbased deep learning framework,'' Pattern Recognit. Lett., vol. 143, pp. 58–66, Mar. 2021.

[32] M. A. Khan, M. Sharif, T. Akram, R. Damaševićius, and R. Maskeliunas, ¯ ''Skin lesion segmentation and multiclass classification using deep learning features and improved moth flame optimization,'' Diagnostics, vol. 11, no. 5, p. 811, Apr. 2021.

[33] A. Mahbod, G. Schaefer, C. Wang, G. Dorffner, R. Ecker, and I. Ellinger, ''Transfer learning using a multi- scale and multi-network ensemble for skin lesion

classification,'' Comput. Methods Programs Biomed., vol. 193, Sep. 2020, Art. no. 105475.

[34] T. Akram, H. M. J. Lodhi, S. R. Naqvi, S. Naeem,

M. Alhaisoni, M. Ali, S. A. Haider, and N. N. Qadri, ''A multilevel features selection framework for skin lesion classification,'' Hum.-Centric Comput. Inf. Sci., vol. 10, no. 1, pp. 1–26, Dec. 2020.

[35] J. Amin, A. Sharif, N. Gul, M. A. Anjum, M. W. Nisar, F. Azam, and S. A. C. Bukhari, ''Integrated design of deep features fusion for localization and classification of skin cancer,'' Pattern Recognit. Lett., vol. 131, pp. 63–70, Mar. 2020.

[36] M. Zhang, W. Li, R. Tao, H. Li, and Q. Du, ''Information fusion for classification of hyperspectral and LiDAR data using IP-CNN,'' IEEE Trans. Geosci. Remote Sens., vol. 60, pp. 1–12, 2022.

[37] X. Li, W. Li, and R. Tao, ''Staged detection– identification framework for cell nuclei in histopathology images,'' IEEE Trans. Instrum. Meas., vol. 69, no. 1, pp. 183–193, Jan. 2020.

[38] X. Wei, W. Li, M. Zhang, and Q. Li, ''Medical hyperspectral image classification based on end-to-end fusion deep neural network,'' IEEE Trans. Instrum. Meas., vol. 68, no. 11, pp. 4481–4492, Jan. 2019.

[39] J. L. Shih and L. H. Chen, ''Colour image retrieval based on primitives of colour moments,'' IEE Proc.- Vis., Image Signal Process., vol. 149, no. 6, pp. 370– 376, Dec. 2002.

[40] V. Patel, S. Shah, H. Trivedi, and U. Naik, ''An analysis of lung tumor classification using SVM and ANN with GLCM Features,'' in Proc. 1st Int. Conf. Comput., Commun., Cyber-Secur. (IC4S). Singapore: Springer, 2020, pp. 273–284.

[41] S. Tiwari, ''A blur classification approach using deep convolution neural network,'' Int. J. Inf. Syst. Model. Design, vol. 11, no. 1, pp. 93–111, Jan. 2020.

[42] S. Tiwari, ''A comparative study of deep learning models with handcraft features and non-handcraft features for automatic plant species identification,'' Int.

J. Agricult. Environ. Inf. Syst., vol. 11, no. 2, pp. 44–57, Apr. 2020.

[43] S. Tiwari, ''An analysis in tissue classification for colorectal cancer histology using convolution neural network and colour models,'' Int. J. Inf. Syst. Model. Design, vol. 9, no. 4, pp. 1–19, Oct. 2018.

[44] H. Li, X. Wang, C. Liu, Y. Wang, P. Li, H. Tang,

L. Yao, and H. Zhang, ''Dual-input neural network integrating feature extraction and deep learning for coronary artery disease detection using electrocardiogram and phonocardiogram,'' IEEEAccess, vol. 7, pp. 146457–146469, 2019.

[45] P. Tschandl, C. Rosendahl, and H. Kittler, ''The HAM10000 dataset, a large collection of multi-source dermatoscopic images of common pigmented skin lesions,'' Sci. Data, vol. 5, no. 1, Dec. 2018, Art. no. 180161.

[46] N. C. F. Codella, D. Gutman, M. E. Celebi, B. Helba, M. A. Marchetti, S. W. Dusza, A. Kalloo, K. Liopyris, N. Mishra, H. Kittler, and A. Halpern, ''Skin lesion analysis toward melanoma detection: A challenge at the 2017 international symposium on biomedical imaging (ISBI),'' in Proc. 15th Int. Symp. Biomed. Imag. (ISBI) 2018, pp. 168–172.

[47] A. K. Sharma, G. Aggarwal, S. Bhardwaj, P. Chakrabarti, T. Chakrabarti, J. H. Abawajy, S. Bhattacharyya, R. Mishra, A. Das, and H. Mahdin, ''Classification of Indian classical music with time- series matching deep learning approach,'' IEEE Access, vol. 9, pp. 102041–102052, 2021.

[48] S. Tiwari, A. Jain, A. K. Sharma, and K. Mohamad Almustafa, ''Phonocardiogram signal based multi-class cardiac diagnostic decision support